

A splicing technique for image tampering using morphological operations



Achmad Fanany Onnilita Gaffar^{a,1}, Supriadi^{a,2}, Arief Bramanto Wicaksono Putra^{a,3}, Rheo Malani^{a,4,*}, Agusma Wajiansyah^{a,5}

^a Department of Information Technology, Politeknik Negeri Samarinda, East Kalimantan, Indonesia

¹ onnygaffar212@gmail.com; ² supriadi.polnes@gmail.com; ³ ariefbram@gmail.com; ^{4,*} anaogie@gmail.com; ⁵ agusma.wajiansyah@gmail.com

* corresponding author

ARTICLE INFO

Article history

Received

Revised

Accepted

Keywords

Image manipulation

Image tampering

Splicing technique

Morphological operations

ABSTRACT

Image tampering is one part of the field of image editing or manipulation that changes certain parts of the graphic content of a given image. There are several techniques commonly used for image tampering, such as splicing, copy-move, retouching, etc. Splicing is a type of image tampering technique that combines two different images, replacing particular objects, skewing, rotation, etc. This study applies the splicing technique to image tampering using morphological operations. Morphology is a collection of image processing operations that process images based on their shape. The aim of this study is to replace particular objects in an original image with other objects that are similar to another selected image. In this study, we try to replace the ball object in the original image with another ball object from another image.

This is an open access article under the [CC-BY-SA](#) license.



1. Introduction

Images are one of the essential tools for carrying information, have been widely studied. Classic image processing is a relatively mature discipline. For classical image processing, relevant technology (e.g. image encryption, the geometric transformation of images, image enhancement, image compression) has developed quite mature [1]. An image is a description of visual perception represented in a two-dimensional picture formation, which resembles a subject - usually a physical object. In the context of signal processing, the image is the distributed color amplitude. In computer science, digital image processing is the use of computer algorithms to do image processing on digital images [2]. Previously, image processing was to improve image quality. It is aimed at humans to enhance people's visual effects. In image processing, the input is lower quality images, and the output is better quality images. Typical image processing includes image enhancement, restoration, encoding and compression. The rapid world of computing, which is marked by the increasing capacity and speed of computer processes, also affects the development of various algorithms, techniques, and methods in the field of image processing. This development gave rise to various application domains utilizing image processing such as feature extraction [3-8], classification [9-12], multi-scale signal analysis [13-17], projection [18, 19], recognition [4, 7, 20, 21]. The rapid development of image processing also accompanied by the emergence of irresponsible actions related to the manipulation and destruction of photos or videos with unfavorable purposes. On the other hand, the manipulation and tampering of photos or videos also done for editing purposes [22]. Image editing or image manipulation is any operation on digital images with the software on a computer or other digital device. Image forgery is image manipulation that produces fake graphic content that falsifies some

facts that happened in the past. Image tampering is a particular type of image forgery that changes parts or portions of the graphic content of a given image [23]. There are various image tampering techniques. Some of them are splicing, copy-move, retouching, resampling, and enhancement [24]. However, splicing and copy-move are the two most commonly used techniques because they completely change the message conveyed by the image [25]. Splicing is the merging of two different images, replacing, skewing, stretching, rotation, etc. [26-29], while copy-move is copying part of an image and pasting it to different locations in the same image.

Image manipulation has an impact on changes in the quality of the intended image. Image quality is defined as a combination of three factors: fidelity, perception and aesthetics. Fidelity is the accuracy of the image which is distorted relative to the original image. Perception is inspired by the characteristics of the human visual system (HVS). This type of metric considers for example visual attention, contrast masking, etc. Aesthetics are subjective and may contain visual constancy, visual attention, visual fatigue, etc. [30]. This study applies the splicing technique for image tampering using morphological operations. The aim is to replace a circle object in an image with another circle object from another image.

2. Methods

In this study, we try to replace the ball object in the original image with another similar object from another image. In general, the method used is shown in Fig. 1. This section will briefly describe each stage of the method used.

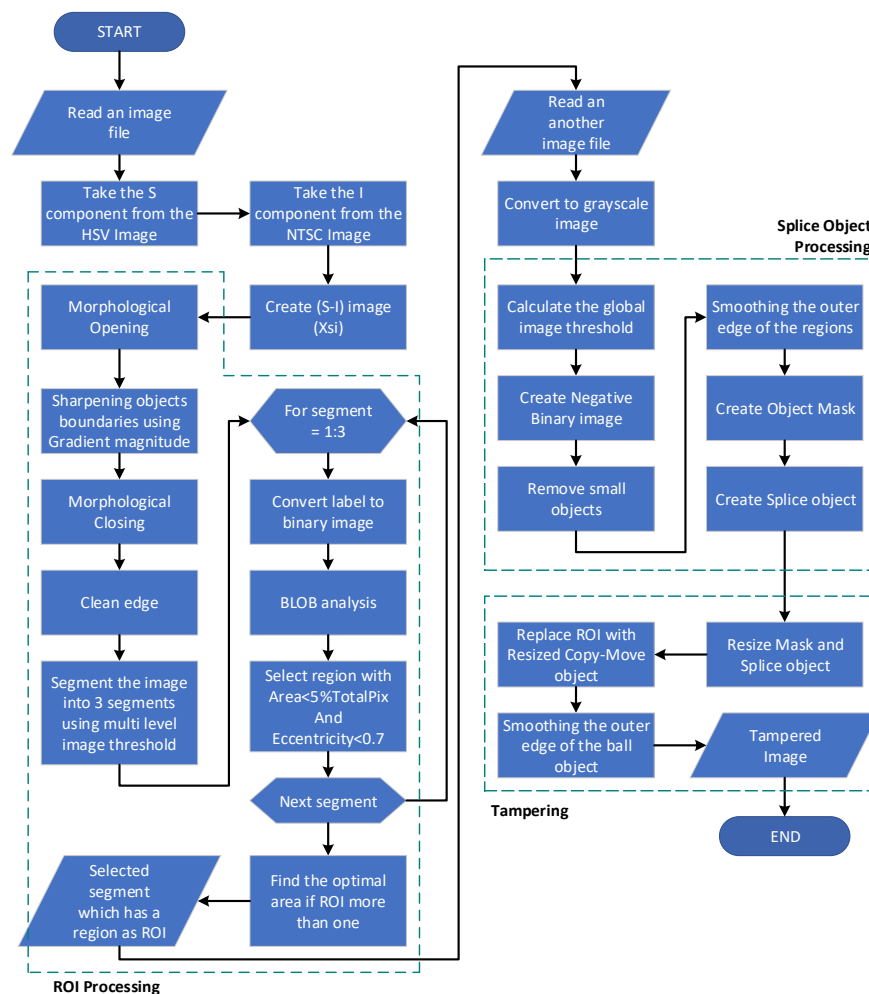


Fig. 1. The Proposed Method

2.1. Create $S-I$ image

The image that will be tampered is a true-color image. The first time, the image changed into two-color maps, HSV, and NTSC. The S (Saturation) component of the HSV image subtracted from the component I (hue) of the NTSC image. This technique is used to obtain a sharpened gray image. The results shown in Fig. 2.

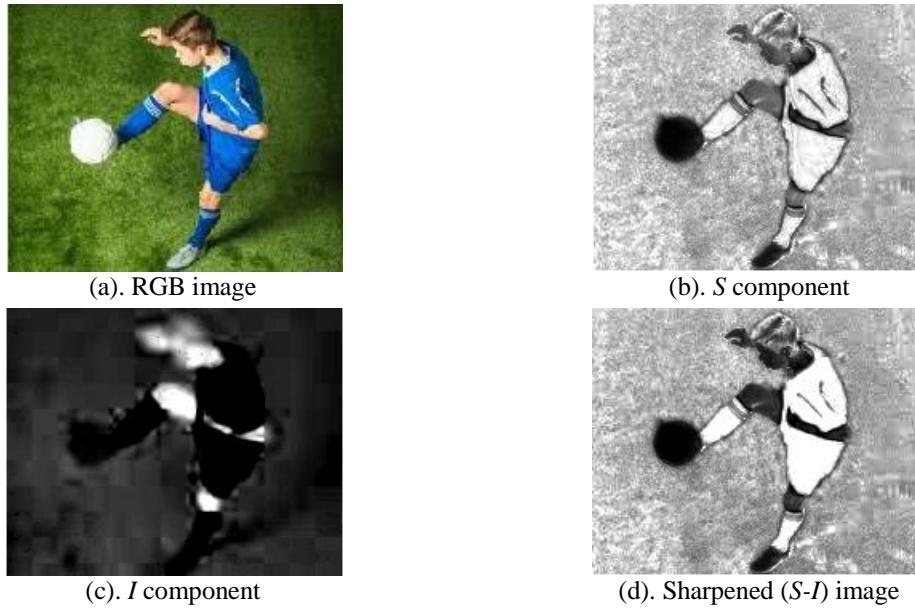


Fig. 2. The sharpened ($S-I$) image

2.2. ROI Processing

This stage is to obtain the Region of Interest (ROI) from the original image to be tampered. The sequence of steps is as follows.

1) Morphological operations

ROI is the part of the image that will be filtered for further operations. ROI is selected using a Binary Mask, which is a binary image whose size is the same as ROI, where pixels that are part of the ROI set to 1, and others set to 0. Binary masks are created using morphological operations.

Morphology is a collection of image processing operations that process images based on their shape. Morphological operations on images can be used for: (1). object extraction; (2). Image filtering, (3). Image segmentation; (4). Measurements, such as texture analysis and shape description. There are two basic operations of morphology, dilation, and erosion. Dilation operations add pixels to the boundaries of objects in an image, whereas erosion operations are the opposite. The number of pixels added or removed from objects in the image depends on the size and shape of the structuring element used. The basic rules of dilation and erosion operations are as follows: (1). Dilation: output pixel is the maximum value of neighboring pixels bounded by structural elements; (2). Erosion: output pixels are the minimum values of neighboring pixels that are bounded by structural elements. A structural element is a matrix consisting of only 0 and 1, which can have arbitrary shapes and sizes, where a pixel of value 1 defines a neighborhood. Structuring elements can be thought of as neighboring pixel blocks applied to each pixel of the image using a sliding neighborhood operation. The observed image pixel positioned in the center of a neighboring block, where all pixels covered by structural elements that valued as 1 are neighboring pixels. An example is shown in Fig. 3.

Morphological operations of dilation and erosion are not always an inversion. Erosion morphological operations on dilated images may produce images that differ from the original before dilation. The dilated morphological operation followed by erosion is called the Closing morphological operation. In contrast, erosion morphological operations that continue with dilation are called Opening morphological operations.

Morphological closing is used to fill the gaps between object boundaries to smooth the outer edges. The morphological opening is used to suppress all unwanted pixels. Some applications are to emphasize the outer edges between objects and remove unwanted small objects.

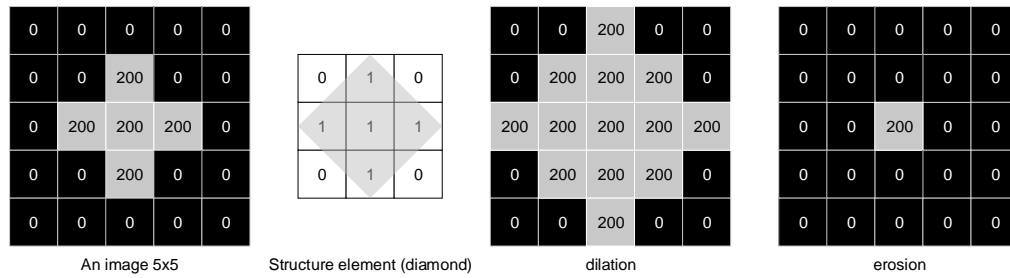


Fig. 3. An example of a morphological operation: dilation and erosion

At this stage, the operation of morphological opening and closing are used to obtain the foreground. These operations use the 'disk' morphological structuring element. Sharpening the boundaries of objects in the image needs to be done before the morphological closing operation. The aim is to emphasize the objects in the image. The results of morphological opening operation shown in Fig. 4.

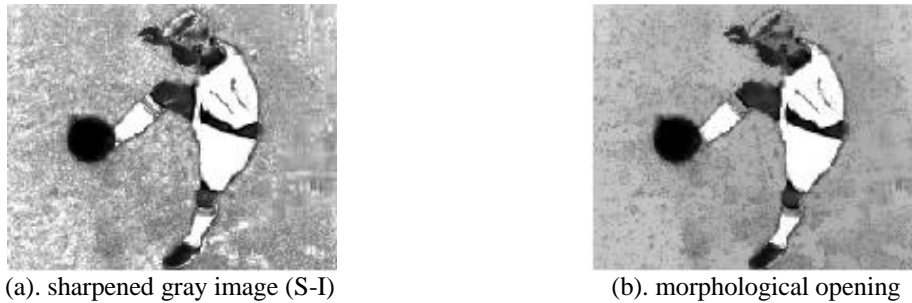


Fig. 4. The results of morphological opening operation

2) Sharpening objects boundaries

The boundaries of each object in the gray image resulting from morphological opening operations need to be emphasized. Sharpening object boundaries is done by utilizing an image of the first-order differential-based edge detection approach, the Sobel edge detection algorithm. The Sobel 3 X 3 kernel convolution operation produces two gradient images, namely vertical and horizontal gradient images. The magnitude gradient of the two images represents the average weight of the difference in the intensity of the image in the neighboring observation pixel. Suppose $P(x, y)$ is the pixel to be observed. The magnitude gradient of this pixel mathematically stated by [31]:

$$\begin{aligned}
 K_X &= \begin{bmatrix} 1 & 0 & -1 \\ 2 & 0 & -2 \\ 1 & 0 & -1 \end{bmatrix} & K_Y &= \begin{bmatrix} 1 & 2 & 1 \\ 0 & 0 & 0 \\ -1 & -2 & -1 \end{bmatrix} \\
 P_X &= P(x, y) * K_X & P_Y &= P(x, y) * K_Y \\
 P_G &= \sqrt{P_X^2 + P_Y^2}
 \end{aligned} \tag{1}$$

Suppose $I_O(x, y)$ is the gray image resulting from morphological opening operation, then the objects boundaries sharpening is stated by:

$$I_G = I_O(x, y) + \frac{P_G}{\max(P_G)} \tag{2}$$

The results shown in Fig. 5. Next, a morphological closing operation is applied to obtain the foreground.

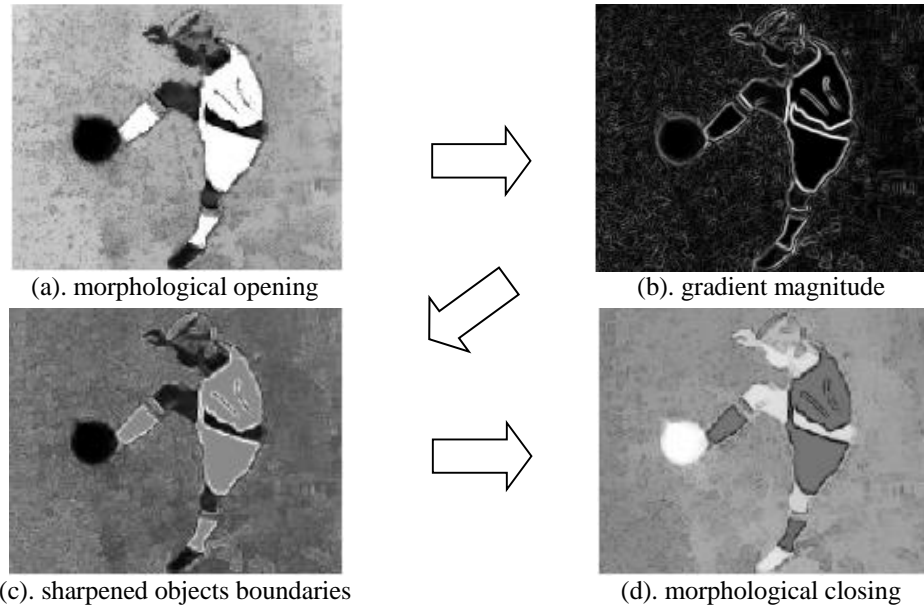


Fig. 5. The results of objects boundaries sharpening using gradient magnitude and morphological closing

3) Clean edge

In principle, this stage aims to emphasize the edge of the region in the image. This is done by applying morphological operations of dilation and erosion sequentially using the rectilinear element structure. The results shown in Fig. 6 (b).

4) Segmentation by using multi level image threshold

Thresholding is a simple method for image segmentation. This method can be used to create a binary image, where every pixel smaller than the constant T is replaced by 0 and vice versa is replaced by 1. Suppose a grayscale image $I(x, y)$. It can be stated by:

$$I_{bw}(x, y) = \begin{cases} 0 & I(x, y) < T \text{ (black)} \\ 1 & I(x, y) \geq T \text{ (white)} \end{cases} \quad (3)$$

where $I(x, y)$ is a grayscale image and T is a threshold constant. In this study, the image is segmented into 3 segments by using multi-level image threshold based on global threshold. The global threshold (T) was obtained using the Otsu Method [32]. The algorithm is as follows:

1. Get a grayscale image.
2. Calculate histogram and probabilities of each intensity level. If L is the number of histogram bins, then the class probabilities stated by:

$$P_1(k) = \sum_{i=0}^{k-1} p_i \quad P_2(k) = \sum_{i=k}^{L-1} p_i \quad P_1(k) + P_2(k) = 1 \quad (4)$$

3. Calculate the class means by using the following formula:

$$\mu_1(k) = \sum_{i=0}^{k-1} i \cdot p_i / P_1(k) \quad \mu_2(k) = \sum_{i=k}^{L-1} i \cdot p_i / P_2(k) \quad \mu_T = \sum_{i=0}^{L-1} i \cdot p_i \quad (5)$$

4. Set up initial $P_i(0)$ and $\mu_i(0)$.
5. Compute all possible threshold for $k = 1 \dots L$.
6. Update P_i and μ_i .
7. Calculate the two classes variance expressed by:

$$\mu_1^2(k) = \sum_{i=0}^{k-1} (i - \mu_1(k))^2 \cdot p_i / P_1(k) \quad \mu_2^2(k) = \sum_{i=k}^{L-1} (i - \mu_2(k))^2 \cdot p_i / P_2(k)$$

$$\mu_T^2(k) = \sum_{i=0}^{L-1} (i - \mu_T(k))^2 \cdot p_i$$
(6)

8. The desired threshold is when $\mu_T^2(k)$ is maximum. The results shown in Fig. 6 (c).

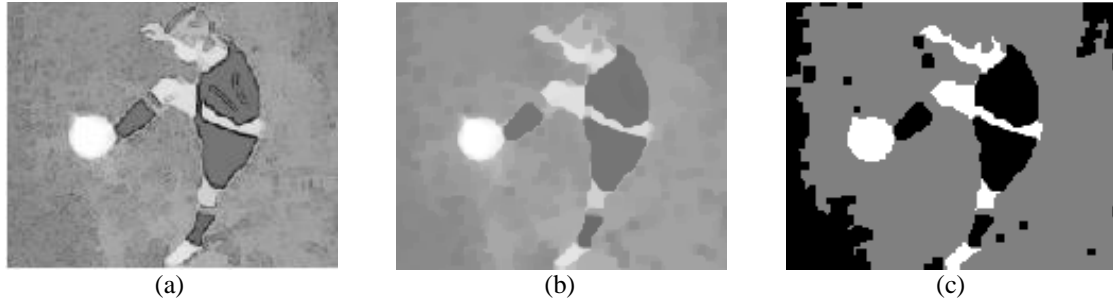


Fig. 6. (a) Morphological closing. (b) Clean edge. (c) image segmentation

5) BLOB analysis

The segmented images are splitted into three binary images based on segmentation labels as shown in Fig. 7. BLOB analysis performed on each binary image to observe the regions that are candidates for ROI. Theoretically, a circle is a region that has an eccentricity of 0, and vice versa line segments have an eccentricity of 1. The circle object in an image can be assumed to have a much smaller number of pixels compared to the total pixel image. In this study, binary images from the segmentation result that have region with eccentricity less than 0.7 and the number of pixels greater than 0.5% and less than 3% of the total pixel image selected as ROI. These values were chosen based on experiments. From Fig. 7, it appears that the binary image that meets the requirements is Segment 3. The BLOB analysis results of Segment 3 shown in Table 1.

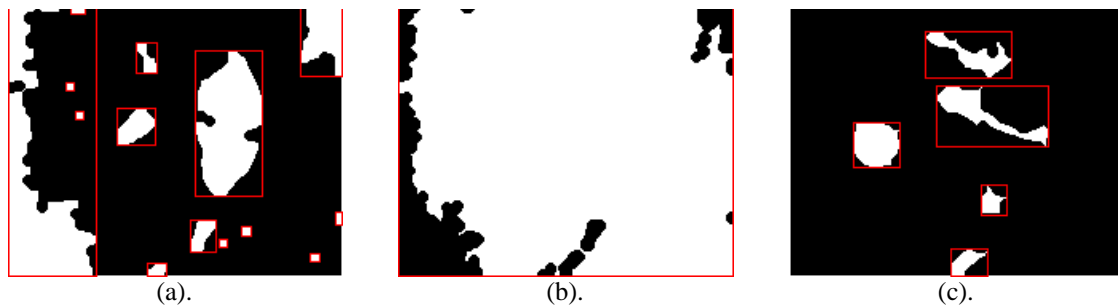


Fig. 7. Binary images from segmented image : (a). Segment 1; (b). Segment 2; (c). Segment 3

Table 1. The BLOB analysis results of Segment 3

Region	BLOB Analysis					A/P
	Eccentricity	Number of pixels in region (P)	Row	Col	Area (A)	
1	0.3524	669	28	29	812	1.2138
2	0.9604	495	54	29	1566	3.1636
3	0.9785	684	38	70	2660	3.8889
4	0.8892	187	17	23	391	2.0909
5	0.5740	151	19	16	304	2.0132

In this study, circle detection uses a comparative between square and circle area approach. A square considered to have rows and columns of the same length. While the circle considered to have a radius of half of the row/column of the square. The area ratio between square and circle is stated by:

$$A_{square} = row^2 \quad A_{circle} = (3.1416) * (0.5 * row)^2$$

$$\frac{A_{square}}{A_{circle}} = 1.2732 \quad (7)$$

Region 1 in Table 1 meets the requirements of Eq. (7) compared to others so that it was chosen as ROI. The results shown in Fig. 8.

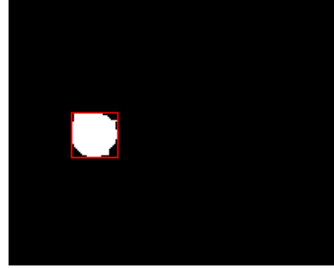


Fig. 8. ROI in Segment 3

2.3. Splice object processing

Different ball object obtained from selected image. The object detection process is the same as the previous steps, with results as shown in Fig. 9(a). The region bounded by red rectangle is the selected object by object mask. The coordinates of the object mask are used as a reference to obtain a splice object from the selected image. The splice object used is intended to replace ball objects in ROI. The coordinates of the object mask are used as a reference to obtain a splice object from the original image. The object mask is then resized as ROI, as is the size of the splice object. The results shown in Fig. 9(b).

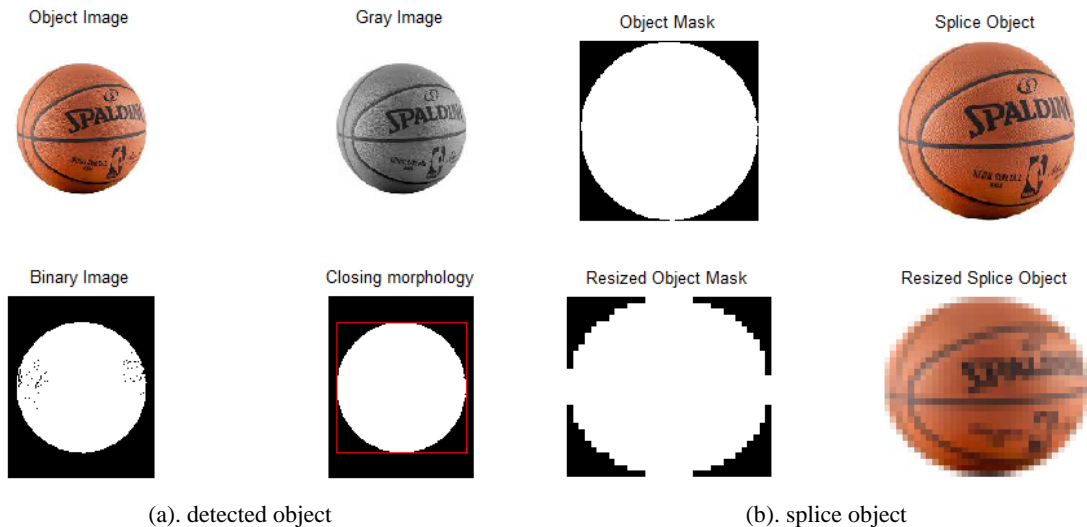


Fig. 9. Create splice object

2.4. Image tampering

The resized object mask dropped to the original image according to the ROI location. The replacement of object in ROI with splice object is done by pixel by pixel inspection. The original pixel value is replaced by the splice object pixel value as long as the resized object mask pixel valued at 1. Probably the results of the tampering image are not smooth. The outer edge of the ball object may contain unexpected pixels. A morphological opening is applied to erase these pixels. The results shown in Fig. 10.

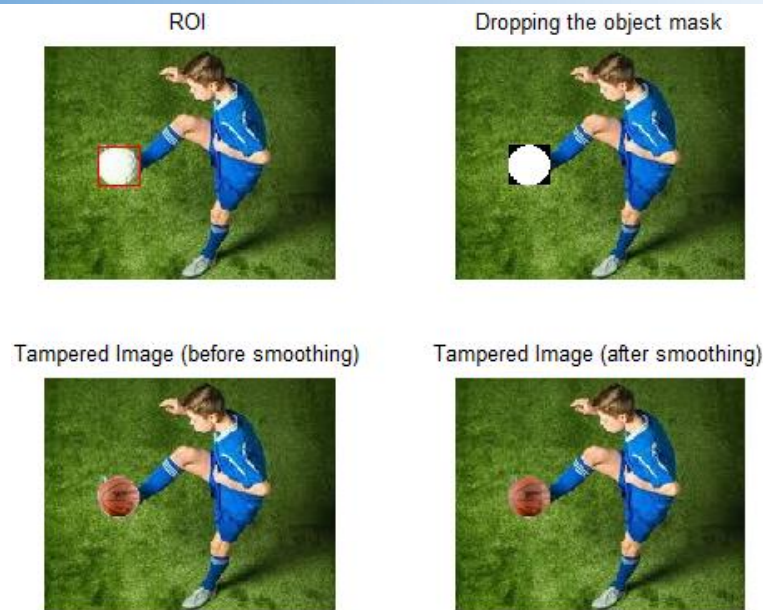


Fig. 10. The result of image tampering

3. Results and Discussion

A more in-depth inspection of Fig. 9 shown in Fig. 10. It could be seen that the tampered image before it smoothed still contains unexpected pixels around the outside edge of the ball object. The presence of these pixels could be affected by the process of changing the size of the splice object to the size of ROI. The final tampered image has obtained after these pixels removed by using a morphological opening.

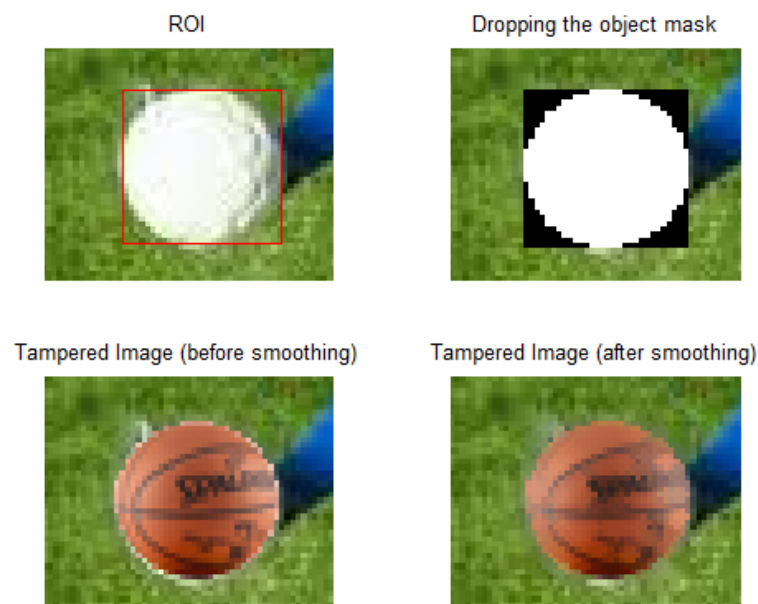
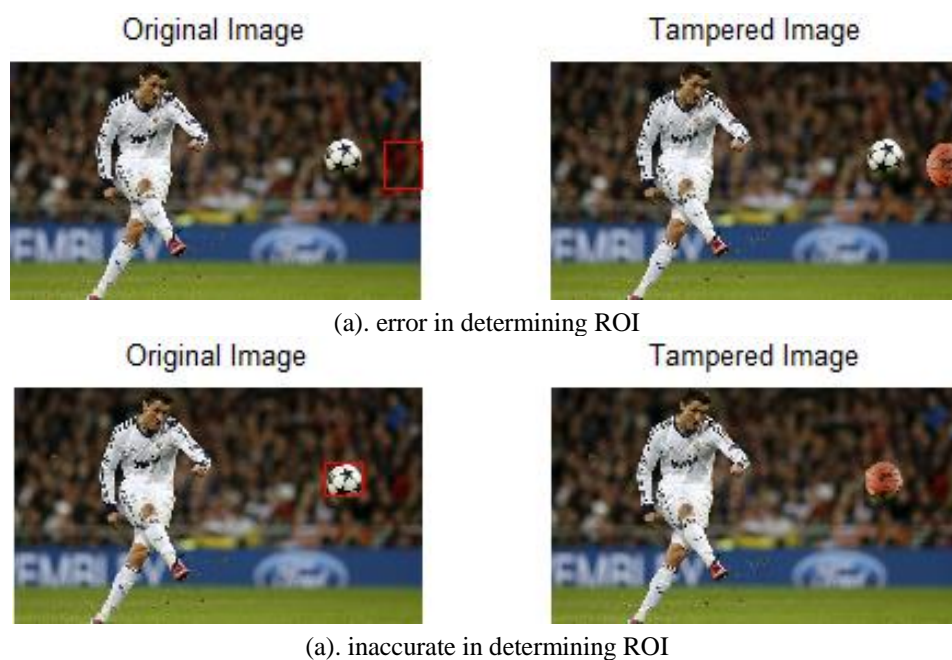


Fig. 11. A more in-depth inspection

One of the disadvantages of this technique, when it is used to smooth the outer edges of a splice object, is that it affects changing the object's content, although it is not so significant — it has shown in Fig. 12. This weakness can facilitate the detection of image splicing that has done.

**Fig. 12.** Changes in object content

The results of tampering are very dependent on the radius value of the 'disk' morphological structuring element used. As an illustration shown in Fig. 13. For some types of images, this method fails to tamper because of an error or inaccurate in determining ROI. As an illustration, shown in Figure 14.

**Fig. 13.** The effect of the radius value of the 'disk' morphological structure elements used on the results of tampering**Fig. 14.** An illustration of the failed tampering

The method has been implemented using a programming tool under the MatLab platform. Several examples of original images have been used to test the method with copy-move objects that picked from selected sample images. The results have shown in Fig. 15.



Fig. 15. The results of the method used implementation

4. Conclusion

This study has applied the splicing technique to image tampering using morphological operations. Research has focused on how to replace a ball object in the original image with another spherical object from another selected image. The method used has applied to several examples of original images where splice objects taken from selected sample images. The difference between the S (Saturation) component of the HSV image and the I (hue) component of the NTSC image has used to get a sharp gray image. The operation of morphological opening and closing have used to obtain the foreground of the sharp gray image. The magnitude gradient of the image resulting from the morphological opening operation has used to sharpen the boundaries of the object before the morphological closing operation. A multi-level image threshold has been applied to segment the sharpened image of the object boundaries into three segments. BLOB analysis has performed on each binary image obtained from the separation of segmented images based on their labels. Finally, a region that has an eccentricity value of less than 0.7, the number of pixels greater than 0.5% and smaller than 3% of the total pixels, and which has the lowest ratio of the square area against the number of pixels chosen as ROI.

The results of the study showed that visually tampered images were quite good. The appearance of unexpected pixels affected by the process of changing the size of the splice object mask to the size of the ROI has corrected using a morphological opening. One disadvantage of this technique, when used to smooth the outer edges of splice objects, is that it affects changing the object's content,

although it is not so significant, so it is easily detected. The results of the study also showed that the results of the tampering process were highly dependent on the value of the radius of the structural elements of the 'disk' morphology used. Besides, for some image types, this method fails to tamper because of errors or inaccuracies in determining ROI.

Further studies will improve results through more in-depth inspection around ROI, especially for the refinement process in such a way that it does not affect the changing content of the object. Besides, the method will also be improved so that it can be applied to all types of images.

References

- [1] P. Li and Y. Zhao, "A Simple Encryption Algorithm for Quantum Color Image," *International Journal of Theoretical Physics*, vol. 56, pp. 1961-1982, 2017.
- [2] P. Chakravorty, "What Is a Signal?," *IEEE Signal Processing Magazine*, 2018.
- [3] L. G. Hafemann, R. Sabourin, and L. S. Oliveira, "Writer-independent Feature Learning for Offline Signature Verification using Deep Convolutional Neural Networks," *International Joint Conference on Neural Networks (IJCNN)*, Vancouver, BC, Canada, IEEE, 2016.
- [4] E. Hussain, A. Hannan, and K. Kashyap, "A Zoning based Feature Extraction method for Recognition of Handwritten Assamese Characters " *International Journal of Computer Science and Technology*, vol. 6, 2015.
- [5] M. R. Kaur and M. P. Choudhary, "Handwritten Signature Verification Based on Surf Features Using HMM," *International Journal of Computer Science Trends and Technology (IJCT)*, vol. 3, 2015.
- [6] F. S. Mohamad, F. M. Alsuhiat, Mohamad Afendee Mohamed, M. Mohamad, and A. A. Jamal, "Detection and Feature Extraction for Images Signatures," *International Journal of Engineering & Technology*, vol. 7, 2018.
- [7] M. A. Mohamad, D. Nasien, H. Hassan, and H. Haron, "A Review on Feature Extraction and Feature Selection for Handwritten Character Recognition," *(IJACSA) International Journal of Advanced Computer Science and Applications*, vol. 6, 2015.
- [8] S. T. Panchal and V. V. Yerigeri, "Offline signature verification based on geometric feature extraction using artificial neural network," *IOSR Journal of Electronics and Communication Engineering (IOSR-JECE)*, vol. 13, 2018.
- [9] A. J. S, P. C. R, T. V, S. K, K. B. Raja, D. Anvekar, V. K. R, S. S. Iyengar, L. M. Patnaik, A. C, and P. K. S, "OSPCV: Off-line Signature Verification using Principal Component Variances " *IOSR Journal of Computer Engineering (IOSR-JCE)*, vol. 7, 2015.
- [10] J. J. d. M. Sá Junior, L. C. Ribas, and O. M. Bruno, "Randomized neural network based signature for dynamic texture classification," *Expert Systems with Applications*, vol. 135, pp. 194-200, 2019.
- [11] Y. Serdouk, H. Nemmour, and Y. Chibani, "Handwritten signature verification using the quad-tree histogram of templates and a Support Vector-based artificial immune classification," *Image and Vision Computing*, vol. 66, pp. 26-35, 2017.
- [12] P. Wei, H. Li, and P. Hu, "Inverse Discriminative Networks for Handwritten Signature Verification," *Computer Vision and Pattern Recognition (CVPR)*, IEEE Xplore, 2019.
- [13] H.-H. Chao, C.-W. Yeh, C. F. Hsu, L. Hsu, and S. Chi, "Multiscale Entropy Analysis with Low-Dimensional Exhaustive Search for Detecting Heart Failure," *Applied Sciences*, vol. 9, p. 3496, 2019.
- [14] H. Ding, X. Jiang, B. Shuai, A. Q. Liu, and G. Wang, "Context Contrasted Feature and Gated Multi-scale Aggregation for Scene Segmentation," *CVF Conference on Computer Vision and Pattern Recognition*, IEEE Computer Society, 2018.
- [15] X. Shen and A. I. Zayed, "Continuous Non-negative wavelets and their use in Density Estimation," *researchgate, publication no.267003753*, 2013.
- [16] L. Xing, L. Cai, H. Zeng, J. Chen, J. Zhu, and J. Hou, "A multi-scale contrast-based image quality assessment model for multi-exposure image fusion," *Signal Processing*, vol. 145, pp. 233-240, 2018.
- [17] L. Yang, X. Chen, and L. Tao, "Acoustic scene classification using Multi-Scale Features," *Detection and Classification of Acoustic Scenes and Events*, Surrey, UK, 2018.

- [18] G. Liang, S. Ren, and F. Dong, "An EIT image segmentation method based on projection distance minimization," *2017 IEEE International Conference on Imaging Systems and Techniques (IST)*, Beijing, China 2017.
- [19] R. Wei, F. Zhou, B. Liu, B. Liang, B. Guo, and X. Xu, "A CNN Based Volumetric Imaging Method With Single X-ray Projection," *2017 IEEE International Conference on Imaging Systems and Techniques (IST)*, Beijing, China, 2017.
- [20] V. Conti, "Biometric Authentication Overview: a Fingerprint Recognition Sensor Description," *International Journal of Biosensors & Bioelectronics*, vol. 2, 2017.
- [21] S. Theodoridis and K. Koutroumbas, *Pattern Recognition - Second Edition*. America: Academic Press - An imprint of Elsevier, 2003.
- [22] S. Mushtaq and A. H. Mir, "Image Copy Move Forgery Detection: A Review," *International Journal of Future Generation Communication and Networking*, vol. 11, pp. 11-22, 2018.
- [23] L. Zheng, Y. Zhang, and V. L. L. Thing, "A survey on image tampering and its detection in real-world photos," *Journal of Visual Communication and Image Representation*, vol. 58, pp. 380-399, 2019.
- [24] S. Mushtaq and A. H. Mir, "Digital Image Forgeries and Passive Image Authentication Techniques: A Survey," *International Journal of Advanced Science and Technology*, vol. 73, pp. 15-32, 2014.
- [25] O. M. Al-Qershi and B. E. Khoo, "Passive detection of copy-move forgery in digital images: state-of-the-art," *Forensic Sci Int*, vol. 231, pp. 284-95, Sep 10 2013.
- [26] AtifShah and E.-S. M. El-Alfy, "Image Splicing Forgery Detection Using DCT Coefficients with Multi-Scale LBP," *2018 International Conference on Computing Sciences and Engineering (ICCSE)*, Kuwait City, Kuwait, 2018.
- [27] A. B and N. George, "A robust technique for splicing detection in tampered blurred images," *2017 International Conference on Trends in Electronics and Informatics (ICEI)*, Tirunelveli, India, 2017.
- [28] N. Pham, J.-W. Lee, G.-R. Kwon, and C.-S. Park, "Hybrid Image-Retrieval Method for Image-Splicing Validation," *Symmetry*, vol. 11, p. 83, 2019.
- [29] H. u. Rhhman, M. Arif, S. Al-Azani, and V. E. Balas, "Comparative Analysis of various Image Splicing Algorithms " *ResearchGate/publication/335030672*, 2019.
- [30] N. Al Madeed, Z. Awan, and S. Al Madeed, "Image Quality Assessment - A Survey of Recent Approaches," pp. 143-156, 2018.
- [31] M. Mittal, A. Verma, I. Kaur, B. Kaur, M. Sharma, L. M. Goyal, S. Roy, and T.-h. Kim, "An Efficient Edge Detection Approach to Provide Better Edge Connectivity for Image Analysis," *IEEE Access*, vol. 7, 2019.
- [32] M. A. B. Siddique, R. B. Arif, and M. M. R. Khan, "Digital Image Segmentation in Matlab: A Brief Study on Otsu's Image Thresholding," *Creative Commons CC BY license*, doi:10.20944/preprints201811.0530.v2, 2019.